universe

IMPACT FACTOR 2.5

CITESCORE 4.3

Article

The Effective Baryon–Baryon Potential with Configuration Mixing in Quark Models

Xinmei Zhu, Hongxia Huang and Jialun Ping

MDPI

https://doi.org/10.3390/universe10100382

universe

MDPI

Article

The Effective Baryon–Baryon Potential with Configuration Mixing in Quark Models

Xinmei Zhu [1,*], Hongxia Huang [2] and Jialun Ping [2]

[1] Department of Physics, Yangzhou University, Yangzhou 225009, China
[2] Department of Physics, Nanjing Normal University, Nanjing 210023, China; hxhuang@njnu.edu.cn (H.H.); jlping@njnu.edu.cn (J.P.)
* Correspondence: xmzhu@yzu.edu.cn

Abstract: The effective baryon–baryon potential can be derived in the framework of the quark model. The configurations with different quark spatial distributions are mixed naturally when two baryons get close. The effect of configuration mixing in the chiral quark model (ChQM) is studied by calculating the effective potential between two non-strange baryons in the channels $IJ = 01, 10$ and 03. For comparison, the results of the color screening model (CSM) are also presented. Generally, configuration mixing will lower the potential when the separation between two baryons is small, and its effect will be ignorable when the separation becomes large. Due to the screened color confinement, the effect of configuration mixing is rather large, which leads to stronger intermediate-range attraction in the CSM, while the effect of configuration mixing is small in the ChQM due to the quadratic confinement and σ-meson exchange, which is responsible for the intermediate-range attraction.

Keywords: baryon–baryon interaction; quark model; configuration mixing

PACS: 13.75.Cs; 12.39.Pn; 12.39.Jh

check for updates

Citation: Zhu, X.; Huang, H.; Ping, J. The Effective Baryon–Baryon Potential with Configuration Mixing in Quark Models. *Universe* **2024**, *10*, 382. https://doi.org/10.3390/universe10100382

Academic Editor: Fridolin Weber

Received: 1 August 2024
Revised: 19 September 2024
Accepted: 26 September 2024
Published: 29 September 2024

1. Introduction

Great effort has been made in the study of dibaryon states by both theorists and experimentalists since Jaffe's prediction of the H particle [1]. The dibaryon is a color singlet multi-quark system with a sufficiently smaller size and is believed to be a prospective field for studying the strong interaction phenomenology because the dibaryon may provide more information on quantum chromodynamics (QCD), the fundamental theory of strong interaction.

Baryons are well-founded objects. To bind two baryons together to form a dibaryon state is not an easy task, because too few states have been discovered in experiments so far. Deuterons with isospin–spin–parity $IJ^P = 01^+$ are loosely bound states of protons and neutrons, where the separation between two nucleons is rather large. d^* with $IJ^P = 03^+$ is believed to be a compact object of six quarks that was reported by the WASA@COSY collaboration [2]. The primary results of STAR@RHIC favors the existence of dibaryon state $N\Omega$ with $IJ^P = \frac{1}{2}2^+$ [3]. With the advance of experiments, more dibaryon states may be reported.

To bind two baryons, attraction between two baryons is necessary. Thus, the baryon–baryon effective potential is needed. To obtain the baryon–baryon effective potentials from QCD directly is too complicated to be possible. Lattice QCD is believed to the reliable approach and has made some progress in the baryon–baryon effective potential [4,5]. However, the calculation needs huge computation resources and some approximations are also applied. At the hadron level, several baryon–baryon effective potentials are proposed based on the one-boson exchange model [6–11]. The "QCD inspired" quark model is an effective approach to describe the properties of baryons, and it is also applied to derive the baryon–baryon effective potentials [12–21]. In deriving the effective potential, generally, the

quark cluster model is employed, in which the six quarks are grouped into two three-quark clusters and the internal motions of the three-quark cluster are frozen. However, for the compact hexaquark system or if the two baryons are too close, it is reasonable to assume uark delocalization, which is similar to the electron percolation in molecules. In the 1990s, F. Wang and his collaborators developed a model, the quark delocalization color screening model (QDCSM) [22], based on the Glashow-Isuger model. In the QDCSM, two new components were introduced. One is quark delocalization, and another is color screening, taking into account the differences in confinement interaction inside a single baryon and between two color singlet baryons. Quark delocalization in QDCSM is a convenient way to realize specific configuration mixing. The model can give a good description of nucleon–nucleon interactions and a natural explanation of the similarity between molecular force and nuclear force [22]. The CSM is the QDCSM without quark delocalization, which is replaced by configuration mixing in the present work.

By introducing the exchange of Goldstone bosons and their partner σ-meson between quarks, the chiral quark model (ChQM) can also give a good description of nuclear force. So far, configuration mixing is not considered in the ChQM in calculating the baryon–baryon effective potential. In the present work, the effect of configuration mixing in the ChQM is studied by calculating the baryon–baryon effective potentials. To simplify the calculation, we limit our calculation in the two-flavor world, the non-strange system, and only the central interactions are taken into account. The resonating group method (RGM) [21,23,24] is used to perform the calculation. In molecular physics, the configuration interaction is a post-Hartree–Fock linear variational method for solving the non-relativistic Schrödinger equation within the Born–Oppenheimer approximation for a quantum chemical multi-electron system.

This paper is organized as follows. In Section 2, the model Hamiltonian and the symmetry bases are described. In Section 3, the calculation method is presented. The results are given in Section 4 and a conclusion is given in Section 5.

2. Quark Model and Wave Functions

2.1. The Chiral Quark Model

The Salamanca version of the ChQM is chosen as a representative of chiral quark models [25,26]. It has been successfully applied to describe both hadron spectroscopy and nucleon–nucleon interactions. The model details can be found in Refs. [25,26]. Here, only the Hamiltonian in the baryon–baryon sector is given below. Four pieces of potentials are used. The phenomenological color confinement potential is invoked to represent the color confinement of QCD (V_{ij}^{C}). The one-gluon exchange mimics the asymptotic freedom of QCD (V_{ij}^{G}). In the low-energy region, the chiral symmetry of QCD is spontaneously broken, the current quarks acquire masses and turn into constituent quarks, and Goldstone bosons appear and can be exchanged between the constituent quarks (V^{π}). The chiral partner of the pion is also included (V^{σ}). The aim of this work is to study the effects of configuration mixing on the baryon–baryon interaction; the non-central interactions are expected to play a minor role in the effects, so they are omitted in the calculation here.

$$
\begin{aligned}
H(6) &= \sum_{i=1}^{6}(m_i + \frac{p_i^2}{2m_i}) - T_c(6) + \sum_{i<j=1}^{6} V_{ij}, \\
V_{ij} &= V_{ij}^C + V_{ij}^G + V_{ij}^\pi + V_{ij}^\sigma \\
V_{ij}^C &= -a_c \lambda_i \cdot \lambda_j (r_{ij}^2 + V_0), \\
V_{ij}^G &= \alpha_s \frac{\lambda_i \cdot \lambda_j}{4} \left[\frac{1}{r_{ij}} - \frac{\pi}{m_i m_j} \left(1 + \frac{2}{3} \sigma_i \cdot \sigma_j \right) \delta(r_{ij}) \right], \\
V_{ij}^\pi &= \frac{g_{ch}^2}{4\pi} \frac{m_\pi^2}{12 m_u^2} \frac{\Lambda^2}{\Lambda^2 - m_\pi^2} m_\pi \left[Y(m_\pi r_{ij}) - \frac{\Lambda^3}{m_\pi^3} Y(\Lambda r_{ij}) \right] \sigma_i \cdot \sigma_j, \\
V_{ij}^\sigma &= -\frac{g_{ch}^2}{4\pi} \frac{\Lambda^2}{\Lambda^2 - m_\sigma^2} m_\sigma \left[Y(m_\sigma r_{ij}) - \frac{\Lambda}{m_\pi} Y(\Lambda r_{ij}) \right].
\end{aligned} \tag{1}
$$

where m_π (m_σ) is the pion (sigma) mass, α_{ch} is the chiral coupling constant related to the πNN coupling constant by $\frac{g_{ch}^2}{4\pi} = \left(\frac{3}{5}\right)^2 \frac{g_{\pi NN}^2}{4\pi} \frac{m_u^2}{m_N^2} = 0.556$, Λ is a cutoff parameter, and $Y(x)$ is the Yukawa function, defined as $Y(x) = \frac{e^{-x}}{x}$. T_c is the kinetic energy of the center of mass. All other symbols have their usual meanings.

2.2. The Color Screening Model

The Hamiltonian of the CSM is the same as that of the ChQM with two modifications. First, there is no π and σ meson exchange; second, the screened color confinement is used between quark pairs resident in different baryons. In the calculation of lattice QCD, the long-range confinement interaction between the interacting quark pair is screened once when the separation between two quarks becomes large [27], so the screened confinement is employed for interacting quark pairs that appear in different baryon orbits. That is,

$$
V_{ij}^c = -a_c \lambda_i \cdot \lambda_j \begin{cases} r_{ij}^2 & \text{if } i,j \text{ occurs in the same baryon orbit;} \\ \frac{1-e^{-\mu r_{ij}^2}}{\mu} & \text{if } i,j \text{ occurs in different baryon orbits.} \end{cases} \tag{2}
$$

The fitted parameters are taken from Ref. [26] and given in Table 1. The absolute nucleon mass is controlled by a constant term, V_0, in the confinement potential that does not affect the baryon–baryon interaction. The model parameters of the CSM are fixed by the spectrum of baryons, and the screening parameter μ is fixed by fitting the NN scattering phase shifts.

Table 1. Model parameters.

Model		**ChQM**	**CSM**
Quarks	b (fm)	0.518	0.603
	m_u (MeV)	313	313
	m_d (MeV)	313	313
Confinements	a_c (MeV·fm^{-2})	46.938	25.13
	μ (fm^{-2})	–	0 or 1.0
	V_0 (fm^2)	−1.297	–
OGE	α_s	0.485	1.54
Goldstone bosons	m_σ (MeV)	675	–
	m_π (MeV)	138	–
	Λ (fm^{-1})	4.2	–

2.3. Wave Functions

The symmetry bases of the wave functions for non-strange six-quark system ($Y = 2$) can be constructed through the group chain [28] such as

$$\begin{array}{ccccccc} [1^n] & [\nu] & [\tilde{\nu}] & [c] & [\mu] & I & J \\ \mathrm{SU}_{24} \supset & \mathrm{SU}_2^x & \times [\mathrm{SU}_{12} \supset & \mathrm{SU}_3^c & \times (\mathrm{SU}_4 \supset & \mathrm{SU}_2^\tau & \times \mathrm{SU}_2^\sigma)], \end{array} \tag{3}$$

The partition of particle numbers (Young diagram) $[\lambda_1\lambda_2\cdots\lambda_f]$ with $\lambda_1 \geq \lambda_2 \geq \ldots \geq \lambda_f$, $\lambda_1 + \lambda_2 + \ldots + \lambda_f = f$ and all λs is an integer, and is used to label the irreducible representation of the permutation group, S_f, and the unitary groups, SU_n, in the configuration space, which is formed by f particles occupying n states. The symmetry basis for six quarks systems has the form

$$\Phi^{\alpha}_{Kmn}(q^6) = \left| \begin{array}{c} [\nu]L^mR^n \\ [c]W[\mu]\beta IJM_IM_J \end{array} \right\rangle. \tag{4}$$

where $\alpha = (IJ)$ are the strong-interaction conserved quantum numbers: the isospin and spin. K denotes the intermediate quantum numbers, $[\nu]$, $[\mu]$, which represent the symmetry of the orbital, spin–isospin SU_4. W represents Weyl tableaux, the component index of color symmetry, $[c]$, and β is the inner multiplicity index in the reduction of $[\mu]$ to $[\tau_I] \times [\sigma_J]$, where $[\tau_I]$ and $[\sigma_J]$ are the partitions corresponding to the isospin I and spin J. The relationship between J and $[\sigma_J]$ is as follows: $J = 0$, 1, 2, 3, $[\sigma_J] = [33]$, $[42]$, $[51]$, $[6]$. I is the isospin and M_I is the third component of the isospin. J is the spin and M_J is the third component of the spin. $[c]$ is fixed to [222] and the one-dimensional representation of color SU_3 due to the color singlet requirement. L and R are left and right Gaussians, the single-particle orbital wave functions in the ordinary quark cluster model:

$$\begin{aligned} |L\rangle &= \left(\frac{1}{\pi b^2}\right)^{3/4} e^{-\frac{1}{2b^2}(r_i - S/2)^2}, \\ |R\rangle &= \left(\frac{1}{\pi b^2}\right)^{3/4} e^{-\frac{1}{2b^2}(r_i + S/2)^2}. \end{aligned} \tag{5}$$

where S is a reference center and b is a baryon size parameter. m and n are the numbers of quarks resident in left and right orbits, respectively. For some interesting sets of quantum numbers, α, the allowed intermediate quantum numbers, K, are listed in Table 2. Where M_I, M_J take their maximum values, the eigenenergies are independent of M_I, M_J. The twenty-seven bases for channel $\alpha = (IJ) = 01$ are shown in Appendix A.

Table 2. The allowed $K = [\nu][\mu]$ for interesting sets of α. The irreducible representation of S_6 is denoted by the partitions.

α	K						
01	[6][44]	[51][321]	[42][51]	[42][33]	[42][2211]	[42][321]	[42][411]
10	[6][33]	[51][321]	[42][51]	[42][33]	[42][2211]	[42][321]	[42][411]
03	[6][33]	[42][33]					

The spatial configurations of quarks are denoted by (mn). Configuration mixing means that different quark spatial distributions will be mixed up. The eigen wave function Ψ^{α} is the linear combination of symmetry bases $\Phi^{\alpha}_{Kmn}(q^6)$ under the cluster approximation,

$$\Psi^{\alpha}(q^6) = \sum_{Kmn} c^{\alpha}_{Kmn} \Phi^{\alpha}_{Kmn}(q^6). \tag{6}$$

The numbers of the coupling channels for $\alpha = (01)$, (10) and (03) are 27, 27 and 10, respectively. In Appendix A, the 27 symmetry bases for $\alpha = (01)$ are shown explicitly.

For different configurations, different orbital symmetries $[\nu]$ are allowed. Because there are only two orbits, the Young diagram at most has two rows, which correspond to partitions [6], [51], [42] and [33]. The results are listed in Table 3.

Table 3. The allowed orbital symmetry $[\nu]$ for a given configuration (mn).

$[\nu]$	L^6	L^5R	L^4R^2	L^3R^3	L^2R^4	LR^5	R^6
[6]	1	1	1	1	1	1	1
[51]	0	1	1	1	1	1	0
[42]	0	0	1	1	1	0	0
[33]	0	0	0	1	0	0	0

3. Calculation Method

To study the baryon–baryon interaction, the Schrödinger equation for the 6-quark system has to be solved:

$$H(6)\Psi^\alpha(q^6) = E^\alpha\Psi^\alpha(q^6), \tag{7}$$

where the eigen wave function Ψ^α is the linear combination of the symmetry bases $\Phi^\alpha_{Kmn}(q^6)$ under the cluster approximation, which was given in the second section. By using Equations (6) and (7), it becomes

$$\sum_{k'}[\langle\Phi^\alpha_{k'}|H(6)|\Phi^\alpha_k\rangle - E^\alpha\langle\Phi^\alpha_{k'}|\Phi^\alpha_k\rangle]c^\alpha_k(q^6) = 0, \tag{8}$$

where k stands for (Kmn). The eigen energy of the system can be obtained by solving the generalized eigen equation. The calculation of the 6-body Hamiltonian matrix elements on the symmetry basis is performed by the well-known fractional parentage expansion technique [28]. First, the 6-body Hamiltonian with pairwise terms is reduced to a 2-body Hamiltonian, for example the Hamiltonian for the fifth and sixth particles, by making use the properties of identical particles. Second, the symmetry basis is separated into two parts, a 4-body part (the 1st to the 4th particles) and 2-body part (the 5th and 6th particles), using the coefficients of fractional parentage. Then, the matrix element of the 6-body Hamiltonian can be reduced to the product of coefficients of fractional parentage, 4-body overlaps and 2-body matrix elements.

$$\langle\Phi^\alpha_k|H|\Phi^\alpha_{k'}\rangle = \sum\binom{6}{2}\langle\Phi^\alpha_k|\alpha_1k_1,\alpha_2k_2\rangle\langle\alpha_1'k_1',\alpha_2'k_2'|\Phi^\alpha_{k'}\rangle\langle\alpha_1k_1|\alpha_1'k_1'\rangle\langle\alpha_2k_2|H_{56}|\alpha_2'k_2'\rangle. \tag{9}$$

where $\langle\alpha_1k_1|\alpha_1'k_1'\rangle$ is the 4-body overlap. $\langle\alpha_2k_2|H_{56}|\alpha_2'k_2'\rangle$ is the two-body matrix element and H_{56} represents the two-body operator for the last pair. $\langle\Phi^\alpha_k|\alpha_1k_1,\alpha_2k_2\rangle$ and $\langle\alpha_1'k_1',\alpha_2'k_2'|\Phi^\alpha_{k'}\rangle$ are the total coefficients of fractional parentage. All the needed coefficients can be obtained from Chen's book [29,30]. For details, one can refer Ref. [28]. As an example, an expression of the matrix element in the configuration of L^3R^3 is given in Appendix B.

4. Results and Discussion

The effective potentials between two baryons in the u, d two-flavor world are calculated in the framework of the ChQM and CSM with configuration mixing. The effective potential is defined as

$$V_{eff}(S) = E_6(S) - E_6(S=\infty) \tag{10}$$

where $E_6(S)$ is the eigen energy of the six-quark system with separation, S, between the left and right Gaussians. Here, we only give some results of a non-strange six-quark system with quantum numbers $IJ = 01$, 10 and 03. In order to check the contribution of the configuration mixing to the effective potentials of the baryon–baryon system, we give the results of configuration L^3R^3 only and those of all-configuration mixing (denoted by L^mR^n) in Figures 1–3. One can see that the effects of configuration mixing on the

effective potentials are different for the two models, and the effects vary with the separation. Generally, configuration mixing will reduce the energy of the system compared with that of the L^3R^3 configuration only, and the effects decrease with the increase in the separation.

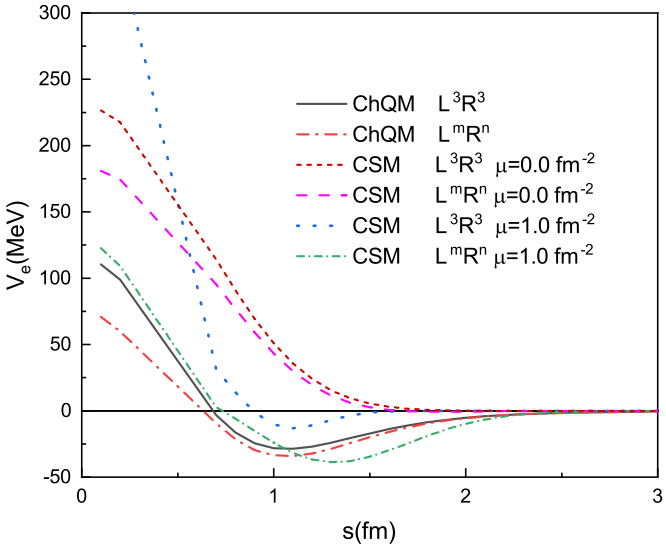

Figure 1. Effective potential (in MeV) vs. baryon-baryon separation (in fm) for N-N ($IJ = 01$) channels.

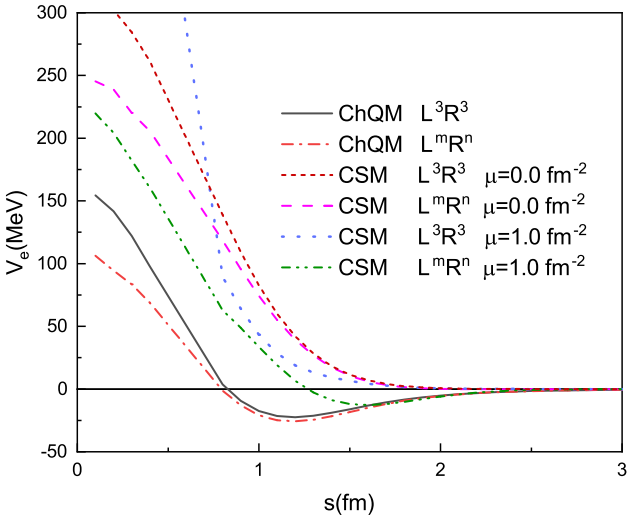

Figure 2. Effective potential (in MeV) vs. baryon-baryon separation (in fm) for N-N ($IJ = 10$) channels.

Figure 1 shows the effective N-N potential for channels $(IJ) = (01)$ with the L^3R^3, configuration comparing it with that under configuration mixing. It is clear that the L^3R^3 configuration only has an effective intermediate-range attraction, but it is a little weaker, ∼5 MeV, than that under configuration mixing in the ChQM. However, in the CSM, configuration mixing has a stronger effective attraction, about 25 MeV, than that under the L^3R^3 configuration only. One can also see that there is no intermediate-range attraction in the CSM if the color screening effect is not taken into account ($\mu = 0.0$ fm^{-2}). The configuration mixing lowers the energy of the system a little, but there is still no attraction. This implies that the quadratic confinement prevents configuration mixing. Only when the confinement is screened can the configuration mixing be developed. The reason can be used to explain the small effects of configuration mixing in the ChQM, where the confinement is not screened and the intermediate-range attraction is mainly provided by the σ-meson exchange. Thus, it is sufficient to use the baryonic structure (L^3R^3) only when studying NN interaction in the ChQM. To see the contribution of different configurations to the

energy of the system at each separation, the percentages of different configurations at a given separation are calculated and are shown in Table 4. From the table, one can see that the baryonic structure (L^3R^3 configuration) is always the main configuration, and it dominates when the separation becomes large in both models. In the ChQM, the L^3R^3 configuration dominates even when the separation is small. The color confinement expels other configurations. It is a good approximation approach to consider only the L^3R^3 configuration in the ChQM. For the CSM, configuration mixing results in an important contribution to the effective potential, and there are considerable non-L^3R^3 configurations in the state when the separation is small, $S \leq 1$ fm. Thus, it is necessary to consider configuration mixing in the CSM.

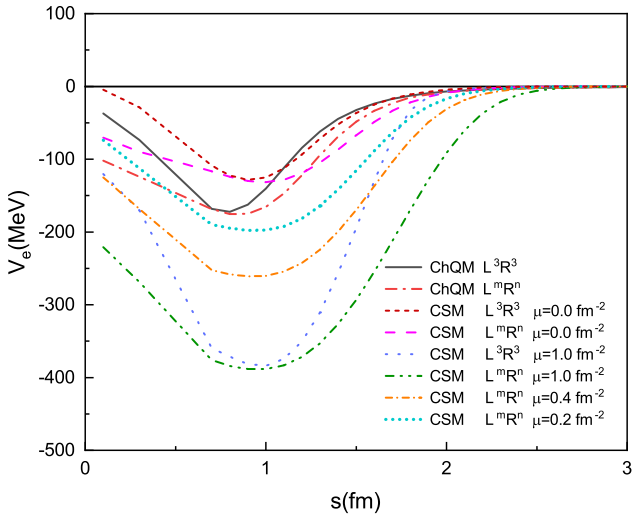

Figure 3. Effective potential (in MeV) vs. baryon-baryon separation (in fm) for Δ-Δ ($IJ = 03$) channels.

Figure 2 shows the effective N-N potential for channels $(IJ) = (10)$. The results are similar to that of $(IJ) = (01)$ (Figure 1). The percentages of different configurations at a given separation are shown in Table 5. The similarity to Table 4 is also apparent.

Figure 3 illustrates the effective Δ-Δ potential for channels $(IJ) = (03)$. Δ-Δ is a decuplet–decuplet channel; many theoretical calculations and some experiments state the existence of the Δ-Δ dibaryon, named d^* [2,24,31,32]. In the ChQM, it is clear that Δ-Δ with the L^3R^3 configuration only has a similar intermediate-range attraction, about 150 MeV, to that of configuration mixing. At a small separation, stronger attraction is obtained with configuration mixing. In the CSM, when color screening is not considered ($\mu = 0.0$ fm^{-2}), modest attractions are obtained in the L^3R^3 configuration only and in configuration mixing calculations. When color screening is considered, $\mu = 1.0$ fm^{-2}, a very strong attraction, ∼400 MeV, appears. The percentages of different configurations at given separations are shown in Table 6. In this case, the L^3R^3 configuration is no longer the main component when the separation is small, and a compact state is expected.

Comparing Figure 3 with the Figures 1 and 2, one can see that there is a deeper intermediate-range attraction between two Δs than that between two nucleons. This can be explained by the structure difference in N compared to Δ. In Δ resonance, the spins of quarks are all parallel, and the color–spin interaction in one-gluon exchange potential gives a positive contribution to the energy of the state, while the spins of quarks in the nucleon are parallel or anti-parallel, half to half, and the color–spin contribution to the energy is negative, so the mass of Δ is larger than that of the nucleon. In the two-baryon system, the contribution of color–spin interaction has more chances to be negative. In addition, configuration mixing lets quarks have more space to move, which lowers the kinetic energy of the system. In this way, ΔΔ systems generally have deeper attraction. From Table 6, one can see that the non-L^3R^3 configurations are still considerable even when the separation is large, $s \sim 1.5$ fm.

Table 4. The percentages of configurations in the states with $IJ = 01$ and $\mu = 1.0$ fm^{-2} (the CSM).

	$s = 0.1$ fm		$s = 0.5$ fm		$s = 1.0$ fm	
	ChQM	**CSM**	**ChQM**	**CSM**	**ChQM**	**CSM**
R^6	0.15	0.15	0.00	0.00	0.00	0.00
R^5L^1	0.00	0.01	0.00	0.08	0.00	0.01
R^4L^2	0.13	0.19	0.17	0.03	0.01	0.12
R^3L^3	0.44	0.30	0.66	0.78	0.78	0.74
R^2L^4	0.13	0.19	0.17	0.03	0.01	0.12
R^1L^5	0.00	0.01	0.00	0.08	0.00	0.01
L^6	0.15	0.15	0.00	0.00	0.00	0.00
	$s = 1.5$ fm		$s = 2.0$ fm		$s = 3.0$ fm	
	ChQM	**CSM**	**ChQM**	**CSM**	**ChQM**	**CSM**
R^6	0.00	0.00	0.00	0.00	0.00	0.00
R^5L^1	0.00	0.00	0.00	0.00	0.00	0.00
R^4L^2	0.00	0.09	0.00	0.00	0.00	0.00
R^3L^3	1.00	0.82	1.00	1.00	1.00	1.00
R^2L^4	0.00	0.09	0.00	0.00	0.00	0.00
R^1L^5	0.00	0.00	0.00	0.00	0.00	0.00
L^6	0.00	0.00	0.00	0.00	0.00	0.00

Table 5. The percentages of configurations in the states with $IJ = 10$ and $\mu = 1.0$ fm^{-2} (the CSM).

	$s = 0.1$ fm		$s = 0.5$ fm		$s = 1.0$ fm	
	ChQM	**CSM**	**ChQM**	**CSM**	**ChQM**	**CSM**
R^6	0.13	0.07	0.00	0.00	0.00	0.00
R^5L^1	0.00	0.00	0.01	0.01	0.00	0.00
R^4L^2	0.14	0.15	0.18	0.22	0.00	0.04
R^3L^3	0.46	0.56	0.63	0.54	1.00	0.92
R^2L^4	0.14	0.15	0.18	0.22	0.00	0.04
R^1L^5	0.00	0.00	0.01	0.01	0.00	0.00
L^6	0.13	0.07	0.00	0.00	0.00	0.00
	$s = 1.5$ fm		$s = 2.0$ fm		$s = 3.0$ fm	
	ChQM	**CSM**	**ChQM**	**CSM**	**ChQM**	**CSM**
R^6	0.00	0.00	0.00	0.00	0.00	0.00
R^5L^1	0.00	0.00	0.00	0.00	0.00	0.00
R^4L^2	0.00	0.04	0.00	0.00	0.00	0.00
R^3L^3	1.00	1.00	1.00	1.00	1.00	1.00
R^2L^4	0.00	0.04	0.00	0.00	0.00	0.00
R^1L^5	0.00	0.00	0.00	0.00	0.00	0.00
L^6	0.00	0.00	0.00	0.00	0.00	0.00

Table 6. The percentages of configurations in the states with $IJ = 03$ and $\mu = 1.0$ fm^{-2} (the CSM).

	$s = 0.1$ fm		$s = 0.5$ fm		$s = 1.0$ fm	
	ChQM	**CSM**	**ChQM**	**CSM**	**ChQM**	**CSM**
R^6	0.29	0.15	0.00	0.00	0.00	0.00
R^5L^1	0.00	0.01	0.02	0.03	0.00	0.01
R^4L^2	0.11	0.19	0.05	0.08	0.05	0.11
R^3L^3	0.20	0.30	0.86	0.78	0.90	0.76
R^2L^4	0.11	0.19	0.05	0.08	0.05	0.11
R^1L^5	0.00	0.01	0.02	0.03	0.00	0.01
L^6	0.29	0.15	0.00	0.00	0.00	0.00

Table 6. *Cont.*

	$s = 1.5$ fm		$s = 2.0$ fm		$s = 3.0$ fm	
	ChQM	**CSM**	**ChQM**	**CSM**	**ChQM**	**CSM**
R^6	0.00	0.07	0.00	0.03	0.00	0.00
R^5L^1	0.00	0.01	0.00	0.00	0.00	0.00
R^4L^2	0.00	0.04	0.00	0.00	0.00	0.00
R^3L^3	1.00	0.76	1.00	0.94	1.00	1.00
R^2L^4	0.00	0.04	0.00	0.00	0.00	0.00
R^1L^5	0.00	0.01	0.00	0.00	0.00	0.00
L^6	0.00	0.07	0.00	0.03	0.00	0.00

5. Summary

By taking into account configuration mixing in the framework of the ChQM and CSM, we calculate the effective potentials of the system such as $NN\ IJ = 01, 10$, as well as the $\Delta\Delta\ IJ = 03$. It can be seen that configuration mixing will reduce the energy of the system, which leads to stronger intermediate-range attraction in both models. Although the effect of configuration mixing is not important in the ChQM, it is indispensable in the CSM. If the compact six-quark state exists, configuration mixing must be considered in the calculation of the binding energy of the system, even in the ChQM, because the effect of configuration mixing is not small when the separation between two clusters is small. The QDCSM is a simple version of the CSM with configuration mixing; only the l^3r^3 configuration is considered, but the left and right single-particle wave functions are delocalized ones, $l = L + \epsilon R$ and $r = R + \epsilon L$. In this way, all the configurations are taken into account but with only one variational parameter, ϵ. This approach is an economic one, greatly reducing the computational burden. The calculations of deuteron properties and nucleon–nucleon scattering phase shifts in the ChQM [24], where no configuration mixing is considered, and in the QDCSM, where configuration mixing is taken into account in a specific way [32], show that the experimental data can be well described; this fact supports the results of the present work. Compared with the more reliable approach, lattice QCD, one can find that the results obtained by lattice QCD are very similar to the ones obtained by quark models [4,5]; for NN with $IJ = 01, 10$, there are repulsive cores and intermediate attractions and for $\Delta\Delta$ with $IJ = 03$, the potential is attractive at all distances. Thus, phenomenological approaches that are easy to implement and that can also give us deep insights into underlying theory are still needed in the near future.

From the results of the present work, one can see that the three-quark cluster baryon is a good approximation in multi-quark systems, for instance sin-quark systems, in the chiral quark model approach. The results also justify the treatment of two baryon systems at the hadron level, where the baryons are taken as point particles. However, if Goldstone boson exchange is not used, then configuration mixing will play an important role. It seems that configuration mixing plays a similar role to meson exchange, and further study is needed.

Author Contributions: Conceptualization, J.P.; methodology, H.H. and X.Z.; investigation, X.Z.; writing—original draft preparation, X.Z.; writing—review and editing, H.H. and J.P.; funding acquisition, J.P. All authors have read and agreed to the published version of the manuscript.

Funding: This research was funded by National Natural Science Foundation of China under Contract Nos. 11675080, 11775118, 11535005 and 11865019.

Data Availability Statement: Research data are given in the manuscript.

Conflicts of Interest: The authors declare no conflicts of interest.

Appendix A. The 27 Symmetry Bases, $\Phi^{(IJ)}_{[\nu][\mu]\ mn}$ for the State with $\alpha = (IJ) = (01)$

For a given $\alpha = (IJ)$ value, the bases are determined by couplings of $[c] \times [\mu] \to [\tilde{\nu}]$ and $[\tau_I] \times [\sigma_J] \to [\mu]$.

$$\Phi^{(01)}_{[6][33]\ 60} = \left| \begin{array}{c} [6]L^6 \\ [222]1[33]10101 \end{array} \right\rangle, \quad \Phi^{(01)}_{[6][33]\ 51} = \left| \begin{array}{c} [6]L^5R^1 \\ [222]1[33]10101 \end{array} \right\rangle,$$
$$\Phi^{(01)}_{[6][33]\ 42} = \left| \begin{array}{c} [6]L^4R^2 \\ [222]1[33]10101 \end{array} \right\rangle, \quad \Phi^{(01)}_{[6][33]\ 33} = \left| \begin{array}{c} [6]L^3R^3 \\ [222]1[33]10101 \end{array} \right\rangle,$$
$$\Phi^{(01)}_{[6][33]\ 24} = \left| \begin{array}{c} [6]L^2R^4 \\ [222]1[33]10101 \end{array} \right\rangle, \quad \Phi^{(01)}_{[6][33]\ 15} = \left| \begin{array}{c} [6]L^1R^5 \\ [222]1[33]10101 \end{array} \right\rangle,$$
$$\Phi^{(01)}_{[6][33]\ 06} = \left| \begin{array}{c} [6]R^6 \\ [222]1[33]10101 \end{array} \right\rangle, \tag{A1}$$

$$\Phi^{(01)}_{[51][321]\ 51} = \left| \begin{array}{c} [51]L^5R^1 \\ [222]1[321]10101 \end{array} \right\rangle, \quad \Phi^{(01)}_{[51][321]\ 42} = \left| \begin{array}{c} [51]L^4R^2 \\ [222]1[321]0101 \end{array} \right\rangle,$$
$$\Phi^{(01)}_{[51][321]\ 33} = \left| \begin{array}{c} [51]L^3R^3 \\ [222]1[321]10101 \end{array} \right\rangle, \quad \Phi^{(01)}_{[51][321]\ 24} = \left| \begin{array}{c} [51]L^2R^4 \\ [222]1[321]10101 \end{array} \right\rangle,$$
$$\Phi^{(01)}_{[51][321]\ 15} = \left| \begin{array}{c} [51]L^1R^5 \\ [222]1[321]10101 \end{array} \right\rangle, \tag{A2}$$

$$\Phi^{(01)}_{[42][51]\ 42} = \left| \begin{array}{c} [42]L^4R^2 \\ [222]1[51]10101 \end{array} \right\rangle, \quad \Phi^{(01)}_{[42][51]\ 33} = \left| \begin{array}{c} [42]L^3R^3 \\ [222]1[51]10101 \end{array} \right\rangle,$$
$$\Phi^{(01)}_{[42][51]\ 24} = \left| \begin{array}{c} [42]L^2R^4 \\ [222]1[51]10101 \end{array} \right\rangle. \tag{A3}$$

$$\Phi^{(01)}_{[42][33]\ 42} = \left| \begin{array}{c} [42]L^4R^2 \\ [222]1[33]10101 \end{array} \right\rangle, \quad \Phi^{(01)}_{[42][33]\ 33} = \left| \begin{array}{c} [42]L^3R^3 \\ [222]1[33]10101 \end{array} \right\rangle,$$
$$\Phi^{(01)}_{[42][33]\ 24} = \left| \begin{array}{c} [42]L^2R^4 \\ [222]1[33]10101 \end{array} \right\rangle, \tag{A4}$$

$$\Phi^{(01)}_{[42][2211]\ 42} = \left| \begin{array}{c} [42]L^4R^2 \\ [222]1[2211]10101 \end{array} \right\rangle, \quad \Phi^{(01)}_{[42][2211]\ 33} = \left| \begin{array}{c} [42]L^3R^3 \\ [222]1[2211]10101 \end{array} \right\rangle,$$
$$\Phi^{(01)}_{[42][2211]\ 24} = \left| \begin{array}{c} [42]L^2R^4 \\ [222]1[2211]10101 \end{array} \right\rangle, \tag{A5}$$

$$\Phi^{(01)}_{[42][321]\ 42} = \left| \begin{array}{c} [42]L^4R^2 \\ [222]1[321]10101 \end{array} \right\rangle, \quad \Phi^{(01)}_{[42][321]\ 33} = \left| \begin{array}{c} [42]L^3R^3 \\ [222]1[321]10101 \end{array} \right\rangle,$$
$$\Phi^{(01)}_{[42][321]\ 24} = \left| \begin{array}{c} [42]L^2R^4 \\ [222]1[321]10101 \end{array} \right\rangle, \tag{A6}$$

$$\Phi^{(01)}_{[42][411]\ 42} = \left| \begin{array}{c} [42]L^4R^2 \\ [222]1[411]10101 \end{array} \right\rangle, \quad \Phi^{(01)}_{[42][411]\ 33} = \left| \begin{array}{c} [42]L^3R^3 \\ [222]1[411]10101 \end{array} \right\rangle,$$
$$\Phi^{(01)}_{[42][411]\ 24} = \left| \begin{array}{c} [42]L^2R^4 \\ [222]1[411]10101 \end{array} \right\rangle, \tag{A7}$$

Appendix B. The Matrix Element in the Configuration of L^3R^3

$$\begin{aligned}\langle\Phi^{(01)}_{[6][33]\ 33}|H|\Phi^{(01)}_{[6][33]\ 33}\rangle &= X^{[6][6]}_{[4][2]}\left[\frac{2}{5}C_s\left(\frac{5}{12}f_s\alpha_A+\frac{2}{12}f_A\alpha_s+\frac{5}{12}f_A\alpha_s\right)\right.\\ &\left.+\frac{3}{5}C_A\left(\frac{4}{54}f_s\alpha_s+\frac{30}{54}f_s\alpha_s+\frac{5}{54}f_s\alpha_s+\frac{15}{54}f_A\alpha_A\right)\right] \quad \text{(A8)}\end{aligned}$$

$$\begin{aligned}\langle\Phi^{(01)}_{[6][33]\ 33}|H|\Phi^{(01)}_{[42][51]\ 33}\rangle &= \frac{1}{3}X^{[6][42]}_{[4][2]}\left[-\sqrt{\frac{3}{5}}C_A\left(\frac{\sqrt{40}}{54}f_s\alpha_s+\frac{\sqrt{360}}{54}f_s\alpha_s\right.\right.\\ &\left.\left.-\frac{\sqrt{40}}{54}f_s\alpha_s-\frac{\sqrt{360}}{54}f_A\alpha_A\right)\right], \quad \text{(A9)}\end{aligned}$$

$$\begin{aligned}\langle\Phi^{(01)}_{[42][51]\ 33}|H|\Phi^{(01)}_{[42][51]\ 33}\rangle &= \frac{1}{9}X^{[42][42]}_{[4][2]}\left[C_A\left(\frac{10}{54}f_s\alpha_s+\frac{12}{54}f_s\alpha_s+\frac{8}{54}f_s\alpha_s+\frac{24}{54}f_A\alpha_A\right)\right]\\ &+ \frac{1}{3}X^{[42][42]}_{[31][2]}\left[\frac{3}{5}C_Af_s\alpha_s+\frac{2}{5}C_A\left(\frac{10}{54}f_s\alpha_s+\frac{12}{54}f_s\alpha_s\right.\right.\\ &\left.\left.+\frac{8}{54}f_s\alpha_s+\frac{24}{54}f_A\alpha_A\right)\right]\\ &+ \frac{2}{9}X^{[42][42]}_{[22][2]}\left[\frac{3}{5}C_s\left(\frac{1}{3}f_s\alpha_A+\frac{2}{3}f_A\alpha_s\right)\right.\\ &\left.+\frac{2}{5}C_A\left(\frac{10}{54}f_s\alpha_s+\frac{12}{54}f_s\alpha_s+\frac{8}{54}f_s\alpha_s+\frac{24}{54}f_A\alpha_A\right)\right]\\ &+ \frac{1}{3}X^{[42][42]}_{[22][2]}\left[\frac{1}{5}C_A\left(\frac{1}{3}f_s\alpha_s+\frac{2}{3}f_A\alpha_s\right)\right.\\ &\left.+\frac{4}{5}C_s\left(\frac{10}{54}f_s\alpha_s+\frac{12}{54}f_s\alpha_s+\frac{8}{54}f_s\alpha_s+\frac{24}{54}f_A\alpha_A\right)\right] \quad \text{(A10)}\end{aligned}$$

where $X^{[\nu][\nu']}_{[\nu_1][\nu_2]}$ is the orbital matrix element, and C_k, f_k, α_k, $k = A, s$ are color, isospin and spin matrix elements, respectively. For the operators, $\lambda_5 \cdot \lambda_6$, $\tau_5 \cdot \tau_6$, $\sigma_5 \cdot \sigma_6$, we have the following results:

$$C_A = -\frac{8}{3}, \quad C_s = \frac{4}{3}; \quad f_A = -3, \quad f_s = 1; \quad \alpha_A = -3, \quad \alpha_s = 1 \quad \text{(A11)}$$

References

1. Jaffe, R.L. Perhaps a Stable Dihyperon. *Phys. Rev. Lett.* **1977**, *38*, 195. [CrossRef]
2. Bashkanov, M. et al. [CELSIUS-WASA Collab] Double-Pionic Fusion of Nuclear Systems and the "ABC" Effect: Approaching a Puzzle by Exclusive and Kinematically Complete Measurements. *Phys. Rev. Lett.* **2009**, *102*, 052301. [CrossRef] [PubMed]
3. Adam, J. et al. [STAR Collab] The Proton-Ω correlation function in $Au + Au$ collisions at $\sqrt{s_{NN}} = 200$ GeV. *Phys. Lett. B* **2019**, *790*, 490. [CrossRef]
4. Ishii, N.; Aoki, S.; Hatsuda, T. Nuclear Force from Lattice QCD. *Phys. Rev. Lett.* **2007**, *99*, 022001. [CrossRef] [PubMed]
5. Gongyo, S. et al. [HAL QCD Collab] $d^*(2380)$ dibaryon from lattice QCD. *Phys. Lett. B* **2020**, *811*, 135935. [CrossRef]
6. Machleidt, R.; Holinde, K.; Elster, C. The Bonn Meson Exchange Model for the Nucleon Nucleon Interaction. *Phys. Rep.* **1987**, *149*, 1.
7. Nagels, M.M.; Rijken, T.A.; de Swart, J.J. A potential model for hyperon-nucleon scattering. *Ann. Phys.* **1973**, *79*, 338. [CrossRef]
8. Nagels, M.M.; Rijken, T.A.; de Swart, J.J. Baryon-baryon scattering in a one-boson-exchange-potential approach.I. Nucleon-nucleon scattering. *Phys. Rev. D* **1975**, *12*, 744. [CrossRef]
9. Cottingham, W.N.; Lacombe, M.; Loiseau, B.; Richard, J.M.; Mau, R.V. Nucleon-Nucleon Interaction from Pion-Nucleon Phase-Shift Analysis. *Phys. Rev. D* **1973**, *8*, 800. [CrossRef]
10. Maessen, P.M.M.; Rijken, T.A.; de Swart, J.J. Soft-core baryon-baryon one-boson-exchange models. II. Hyperon-nucleon potential. *Phys. Rev. C* **1989**, *40*, 2226. [CrossRef]

11. Holzenkamp, B.; Holinde, K.; Speth, J. A Meson Exchange Model for the Hyperon Nucleon Interaction. *Nucl. Phys. A* **1989**, *500*, 485. [CrossRef]
12. Oka, M.; Shimizu, K.; Yazaki, K. Hyperon-Nucleon and Hyperon-hyperon Interaction in a Quark Model. *Nucl. Phys. A* **1987**, *464*, 700. [CrossRef]
13. Koike, Y.; Shimizu, K. Yazaki, K. Study of Hyperon-Nucleon and Hyperon-hyperon Interaction in the Flipflop Model. *Nucl. Phys. A* **1990**, *513*, 653. [CrossRef]
14. Shimizu, K. Study of Baryon Baryon Interactions and Nuclear Properties in the Quark Cluster Model. *Rep. Prog. Phys.* **1989**, *52*, 1. [CrossRef]
15. Yazaki, K. *Properties and Interactions of Hyperons*; World Scientific: Singapore, 1994; p. 189.
16. Straub, U.; Zhang, Z.Y.; Bräuer, K.; Faessler, A.; Khadkikar, S.H.; Lübeck, G. Hyperon Nucleon Interaction in the Quark Cluster Model. *Nucl. Phys. A* **1988**, *483*, 686. [CrossRef]
17. Straub, U.; Zhang, Z.Y.; Bräuer, K.; Faessler, A.; Khadkikar, S.B. Binding Energy of the Dihyperon in the Quark Cluster Model. *Phys. Lett. B* **1988**, *200*, 241. [CrossRef]
18. Fujiwara, Y.; Nakamoto, C.; Suzuki, Y. Unified Description of NN and YN Interactions in a Quark Model with Effective Meson-Exchange Potentials. *Phys. Rev. Lett.* **1996**, *76*, 2242. [CrossRef]
19. Fujiwara, Y.; Nakamoto, C.; Suzuki, Y. RGM study of the hyperon-nucleon interaction in the SU(6) quark model.1: Analysis of NN and $\Sigma^+ p$ systems. RGM study of the hyperon-nucleon interaction in the SU(6) quark model.2: Analysis of ΛN-ΣN (I = 1/2) coupled channel system. *Prog. Theor. Phys.* **1995**, *94*, 353. [CrossRef]
20. Nakamoto, C.; Suzuki, Y.; Fujiwara, Y. Entral force of the hyperon-nucleon interaction in the SU(6) quark model. *Prog. Theor. Phys.* **1995**, *94*, 65. [CrossRef]
21. Ping, J.L.; Wang, F.; Goldman, T. Effective baryon baryon potentials in the quark delocalization and color screening model. *Nucl. Phys. A* **1999**, *657*, 95. [CrossRef]
22. Wang, F.; Wu, G.H.; Teng, L.J.; Goldman, T. Quark delocalization, color screening, and nuclear intermediate range attraction. *Phys. Rev. Lett.* **1992**, *69*, 2901. [CrossRef] [PubMed]
23. Buchmann, A.; Yamauchi, Y.; Faessler, A. The electromagnetic form factors of the deuteron in the quark cluster model. *Nucl. Phys. A* **1989**, *496*, 621. [CrossRef]
24. Valcarce, A.; Garcilazo, H.; Fernandez, F.; Gonzalez, P. Quark-model study of few-baryon systems. *Rep. Prog. Phys.* **2005**, *68*, 965. [CrossRef]
25. Valcarce, A.; Gonzalez, P.; Garcilazo, H.; Fernandez, F.; Vento, V. Chiral quark cluster model study of the low-energy baryon spectrum. *Phys. Lett. B* **1996**, *367*, 35. [CrossRef]
26. Entem, D.R.; Fernández, F.; Valcarce, A. Chiral quark model of the NN system within a Lippmann-Schwinger resonating group method. *Phys. Rev. C* **2000**, *62*, 034002. [CrossRef]
27. Born, K.D.; Laermann, E.; Pirch, N.; Walsh, T.F.; Zerwas, P.M. Hadron properties in lattice QCD with dynamical fermions. *Phys. Rev. D* **1989**, *40*, 1653. [CrossRef]
28. Wang, F.; Ping, J.L.; Goldman, T. Extension of fractional parentage expansion to the nonrelativistic and relativistic $SU_f(3)$ dibaryon calculations. *Phys. Rev. C* **1995**, *51*, 1648. [CrossRef] [PubMed]
29. Chen, J.Q.; Wang, P.N.; Lü, Z.M.; Wu, X.B. *Tables of the Clebsh-Gordan, Racah and Subduction Coefficients of $SU(n)$ Groups*; World Scientific: Singapore, 1987.
30. Chen, J.Q.; Wu, X.B.; Gao, M.J. *Tables of the $SU(mn) \supset SU(m) \times SU(n)$ Coefficients of Fractional Parentage*; World Scientific: Singapore, 1991.
31. Bashkanova, M.; Brodsky, S. Novel Six-Quark Hidden-Color Dibaryon States in QCD. *Phys. Lett. B* **2013**, *727*, 438. [CrossRef]
32. Ping, J.L.; Huang, H.X.; Pang, H.R.; Wang, F.; Wong, C.W. Quark models of dibaryon resonances in nucleon-nucleon scattering. *Phys. Rev. C* **2009**, *79*, 024001. [CrossRef]